IOSR Journal of Mathematics (IOSR-JM)
e-ISSN: 2278-0661, p-ISSN: 2278-8727, Volume 22, Issue 6, Ser. I (Nov. – Dec. 2026), PP 01-20
www.iosrjournals.org

Bayesian Survival Analysis Models; A Comparative Simulation Study of Modified Mixture Gamma Process and Dirichlet Process Cox Models with baseline models.

Joy Omeyi Omoha[1,*] Adams Samuel Olorunfemi[2], Zubair Mohammed Anono[2]
[1] *Department of Biostatistics, Faculty of Science; Federal University of Health Sciences, Otukpo, Nigeria*
[2] *Department of Statistics, Faculty of Science; University of Abuja, Gwagwalada. Nigeria*

Abstract
Background: *Lassa fever remains an important public-health challenge in Nigeria, where recurrent outbreaks, substantial mortality, incomplete follow-up, and heterogeneous clinical trajectories complicate the analysis of patient survival. Conventional survival models, including exponential, Weibull, and Cox proportional hazards models, may be restrictive when the underlying hazard varies over time or when covariate effects are heterogeneous and nonlinear. Bayesian survival methods provide a flexible framework for incorporating uncertainty and prior information, but their application to Lassa fever survival modelling remains limited Survival models often struggle to capture complex hazard shapes, unobserved heterogeneity (frailty), and non-proportional hazards inherent in clinical data. While flexible Bayesian semi-parametric approaches have been proposed to address these limitations, their relative performance in diverse data landscapes remains understudied. This study evaluates two novel frameworks: the Modified Mixture Gamma Process Model (MMGPM) and the Modified Dirichlet Process Cox Model (MDPCM) , comparing them against traditional baseline approaches.*
Objective: *This study develops and evaluates two flexible Bayesian survival models—the* ***Modified Mixture Gamma Process Model (MMGPM)*** *and the* ***Modified Dirichlet Process Cox Model (MDPCM)****—and compares their performance with Bayesian exponential and Weibull models under varying hazard structures, sample sizes, and censoring levels.*
Methods: *A Monte Carlo simulation study was conducted using piecewise exponential survival mechanisms representing homogeneous hazards, heterogeneous time-varying hazards, and nonlinear covariate effects. Sample sizes of 100, 200, and 500 were considered, together with censoring proportions of 20%, 40%, and 60%. Each simulation configuration was replicated 500 times. Model performance was assessed using bias, mean squared error (MSE), empirical 95% credible-interval coverage, concordance index (C-index), and Deviance Information Criterion (DIC). Bayesian estimation was based primarily on Markov Chain Monte Carlo methods, with Integrated Nested Laplace Approximation considered as a computational sensitivity approach.*
Results: *Under homogeneous hazards, the Bayesian exponential model produced the lowest bias and MSE because its constant-hazard assumption coincided with the data-generating mechanism. However, the proposed models remained well calibrated. Under heterogeneous hazards, MMGPM and MDPCM substantially outperformed the conventional models. In the aggregated heterogeneous-hazard scenarios, MMGPM achieved an average bias of 0.0014, MSE of 0.000014, 95% coverage of 0.948, and C-index of 0.759, compared with 0.0038, 0.000041, 0.901, and 0.712, respectively, for the Bayesian exponential model. MDPCM provided the strongest uncertainty calibration, with 95% coverage of 0.961. Similar advantages were observed under nonlinear covariate effects. Across sample sizes, model accuracy improved with increasing sample size, while the proposed models maintained superior performance relative to the conventional baselines.*
Conclusion: *The simulation evidence indicates that MMGPM and MDPCM provide more flexible and robust approaches to survival modelling when hazards are heterogeneous, time-varying, or affected by complex covariate structures. MMGPM demonstrated a particular advantage in point estimation and discrimination, whereas MDPCM provided stronger posterior calibration. These findings support further validation of the proposed models using individual-level Lassa fever survival data from Nigeria.*
Keywords: *Lassa fever; Bayesian survival analysis; Modified Mixture Gamma Process Model; Modified Dirichlet Process Cox Model; Dirichlet process; MCMC, censoring.*

Date of Submission: 27-10-2026 Date of Acceptance: 07-11-2026

I. Introduction

Bayesian survival analysis has emerged as a robust alternative to traditional methods, offering significant advantages such as the ability to incorporate prior knowledge, quantify uncertainty, in resource-limited settings

like Nigeria, data may be sparse or noisy. A Bayesian framework allows incorporating prior knowledge, handling censoring more effectively, and providing probabilistic interpretations of survival outcomes. and handle complex data structures (Bartos *et al*., 2022). Existing Bayesian methods, while powerful, often require significant computational resources and expertise, limiting their accessibility in resource-constrained settings where the disease burden is highest (Bhattacharya & Tyagi 1990). Furthermore, current Bayesian survival models frequently lack disease-specific modifications, reducing their applicability to the unique clinical and epidemiological features of Lassa fever (Guure &Ibrahim 2012; Biard *et al*., 2021). The inadequacies of both frequentist and existing Bayesian survival models underscore the need for a modified Bayesian framework tailored to in the Nigerian context of Lassa fever. Such a framework must address the challenges posed by data sparsity, right-censoring, and incomplete records while incorporating spatial and temporal variations in disease patterns. Additionally, there is a critical need to evaluate the performance of these modified Bayesian models against traditional and existing Bayesian methods to establish their utility in predicting survival outcomes and informing intervention strategies (Stevenson & Brewer, 2017).

While advances in clinical care and public health surveillance have improved outcomes in recent years, critical gaps remain in understanding survival patterns and the factors influencing outcomes in Lassa fever patients, especially under conditions of data sparsity and censoring (Bartoš *et al*., 2022). Bayesian survival analysis offers a flexible framework to address these challenges by incorporating prior knowledge and quantifying uncertainty, making it particularly suitable for diseases like Lassa fever where available data are often limited or incomplete (Bhattacharya & Tyagi, 1990; Renganathan, 2016).

II. Material and Methods

Modified Mixture Gamma Process Model for Baseline Hazard

The MMGPM extends the ordinary gamma-process survival model by allowing each baseline cumulative-hazard increment to arise from one of several latent gamma-process components. This mixture structure is introduced to accommodate unobserved heterogeneity in the underlying hazard.

The derivation proceeds in seven stages.

Step 1: Partition the Follow-up Time

Partition the follow-up period into J non-overlapping intervals

$$I_j = (s_{j-1}, s_j], j = 1,2, \dots, J,$$

with

$$0 = s_0 < s_1 < \cdots < s_J.$$

The cumulative baseline hazard over time is $H_0(t)$. Its increment over interval I_j is defined as

$$h_j = H_0(s_j) - H_0(s_{j-1}). \quad (1)$$

Hence

$$H_0(s_j) = \sum_{\ell=1}^{j} h_\ell. \quad (2)$$

Thus, rather than estimating the entire function $H_0(t)$ directly, the model estimates the sequence of positive increments

$$\mathbf{h} = (h_1, h_2, \dots, h_J)^T.$$

This interval representation provides the basis for introducing the mixture gamma-process structure.

Step 2: Introduce the Mixture Gamma-Process Prior

In the ordinary gamma-process model, all hazard increments are generated from one gamma-process distribution. The MMGPM modifies this assumption by introducing a latent component indicator z_j for each interval.

The model assumes

$$h_j \mid z_j \sim \text{Gamma}\big(c_0 z_j \alpha_0, c_0 z_j\big), z_j \sim \text{Categorical}(\pi_1, \pi_2, \dots, \pi_K). \quad (3)$$

Therefore, the marginal prior distribution of h_j can be expressed as a finite mixture:

$$p(h_j) = \sum_{k=1}^{K} \pi_k \, p(h_j \mid z_j = k).$$

Equivalently,

$$p(h_j) = \sum_{k=1}^{K} \pi_k \text{Gamma}\big(h_j; c_0 k \alpha_0, c_0 k\big). \tag{4}$$

Step 3: Construct the Subject-Specific Hazard

Within interval I_j, let h_{0j} denote the corresponding baseline hazard level. For subject i, the proportional hazards structure becomes

$$h_i(t) = h_{0j} \exp(\mathbf{x}_i^T \boldsymbol{\beta}), t \in I_j. \tag{5}$$

Thus,

$$H_i(t) = \exp(\mathbf{x}_i^T \boldsymbol{\beta}) H_0(t).$$

The survival function is consequently

$$S_i(t) = \exp[-H_0(t) \exp(\mathbf{x}_i^T \boldsymbol{\beta})] \tag{6}$$

This shows explicitly how the gamma-process baseline component and the Cox regression component combine to determine individual survival.

Step 4: Construct the Grouped-Data Likelihood

Let

$$v_{ij} = \begin{cases} 1, & \text{if subject } i \text{ experiences the event in interval } j, \\ 0, & \text{otherwise.} \end{cases}$$

For each subject and interval, the likelihood combines the event contribution and the survival contribution.

The contribution of subject i in interval j is

$$L_{ij} = \big[h_j \exp(\mathbf{x}_i^T \boldsymbol{\beta})\big]^{v_{ij}} \exp\big[-h_j \exp(\mathbf{x}_i^T \boldsymbol{\beta})\big].$$

Taking the product over all n subjects and J intervals gives

$$L(\boldsymbol{\beta}, \mathbf{h} \mid D) = \prod_{i=1}^{n} \prod_{j=1}^{J} \big[h_j \exp(\mathbf{x}_i^T \boldsymbol{\beta})\big]^{v_{ij}} \exp\big[-h_j \exp(\mathbf{x}_i^T \boldsymbol{\beta})\big]. \tag{7}$$

Hence, apart from terms not involving h_j,

$$L(\boldsymbol{\beta}, \mathbf{h} \mid D) \propto \prod_{j=1}^{J} h_j^{d_j} \exp(-R_j h_j).$$

This form is important because it is conjugate with the gamma prior assigned to h_j.

Step 5: Derive the Joint Posterior Distribution

The posterior distribution follows Bayes' theorem:

$$\text{Posterior} \propto \text{Likelihood} \times \text{Prior}.$$

Therefore,

$$\pi(\boldsymbol{\beta}, \mathbf{h}, \mathbf{z}, \boldsymbol{\pi} \mid D) \propto L(\boldsymbol{\beta}, \mathbf{h} \mid D) \, \pi(\mathbf{h} \mid \mathbf{z}) \, \pi(\mathbf{z} \mid \boldsymbol{\pi}) \, \pi(\boldsymbol{\pi}) \, \pi(\boldsymbol{\beta}).$$

Using the interval-specific representation,

Hence, the source model expresses the posterior as

$$\pi(\boldsymbol{\beta}, \mathbf{h}, \mathbf{z} \mid D) \propto L(\boldsymbol{\beta}, \mathbf{h}, \mathbf{z} \mid D) \left[\prod_{j=1}^{J} \pi(h_j \mid z_j) \pi(z_j) \right] \pi(\boldsymbol{\beta}), \tag{8}$$

where

$$\boldsymbol{\beta} \sim N_p(\boldsymbol{\mu}_0, \boldsymbol{\Sigma}_0),$$

and

$$\boldsymbol{\pi} \sim \text{Dirichlet}(\boldsymbol{\delta}).$$

Step 6: Derive the Conditional Posterior of the Hazard Increment

From the likelihood,

$$L_j(h_j \mid D) \propto h_j^{d_j} \exp(-R_j h_j).$$

From the mixture gamma-process prior in Equation (4),

$$\pi(h_j \mid z_j) \propto h_j^{c_0 z_j \alpha_0 - 1} \exp(-c_0 z_j h_j).$$

Multiplying the likelihood and prior gives

$$\begin{aligned} \pi(h_j \mid D, z_j) &\propto h_j^{d_j} \exp(-R_j h_j)\, h_j^{c_0 z_j \alpha_0 - 1} \exp(-c_0 z_j h_j) \\ &= h_j^{c_0 z_j \alpha_0 + d_j - 1} \exp\left[-(c_0 z_j + R_j) h_j\right]. \end{aligned}$$

This is the kernel of a gamma distribution. Therefore,

$$h_j \mid D, z_j \sim \text{Gamma}\left(c_0 z_j \alpha_0 + d_j, c_0 z_j + R_j\right). \tag{9}$$

Thus, the posterior shape parameter is

$$\underbrace{c_0 z_j \alpha_0}_{\text{prior information}} + \underbrace{d_j}_{\text{observed events}},$$

while the posterior rate is

$$\underbrace{c_0 z_j}_{\text{prior precision}} + \underbrace{R_j}_{\text{observed exposure}}.$$

This conjugate structure makes direct Gibbs updating of h_j possible.

Step 7: Posterior Updating of the Latent Mixture Component

Because the component membership z_j is unknown, its posterior probability is obtained using Bayes' rule:

$$P(z_j = k \mid h_j, D) \propto \pi_k\, p(h_j \mid z_j = k).$$

Therefore,

$$P(z_j = k \mid h_j, D) = \frac{\pi_k p(h_j \mid z_j = k)}{\sum_{\ell=1}^{K} \pi_\ell p(h_j \mid z_j = \ell)}. \tag{10}$$

This step assigns each interval probabilistically to one of the K latent hazard components.

If

$$n_k = \sum_{j=1}^{J} I(z_j = k)$$

denotes the number of intervals assigned to component k, conjugacy of the Dirichlet prior gives

$$\boldsymbol{\pi} \mid \mathbf{z} \sim \text{Dirichlet}(\delta_1 + n_1, \delta_2 + n_2, \ldots, \delta_K + n_K).$$

Posterior estimation therefore alternates between updating

$$\mathbf{h}, \mathbf{z}, \boldsymbol{\pi}, \text{ and } \boldsymbol{\beta}.$$

Marginal Likelihood After Integrating Out the Hazard Increment

Because h_j has a conjugate gamma posterior, it can be integrated analytically from the likelihood.

For interval j,

$$L_j(\boldsymbol{\beta}, z_j \mid D) = \int_0^\infty L_j(h_j \mid D)\pi(h_j \mid z_j)\, dh_j.$$

Using the gamma integral identity

$$\int_0^\infty h^{a-1}e^{-bh}\, dh = \frac{\Gamma(a)}{b^a}, a > 0, b > 0,$$

the marginal contribution becomes proportional to

$$\frac{\Gamma\left(c_0 z_j \alpha_0 + d_j\right)}{\left(c_0 z_j + R_j\right)^{c_0 z_j \alpha_0 + d_j}}.$$

Thus, across all intervals,

$$L(\boldsymbol{\beta}, \mathbf{z} \mid D) \propto \prod_{j=1}^{J} \frac{\Gamma\left(c_0 z_j \alpha_0 + d_j\right)}{\left(c_0 z_j + R_j\right)^{c_0 z_j \alpha_0 + d_j}}. \tag{11}$$

The marginal likelihood allows comparison of alternative mixture allocations without explicitly conditioning on each h_j.

Posterior Mean of the Baseline Hazard Increment

For a gamma distribution with shape a and rate b,

$$E(H) = \frac{a}{b}.$$

Applying this result to Equation (3.96),

$$E[h_j \mid D, z_j] = \frac{c_0 z_j \alpha_0 + d_j}{c_0 z_j + R_j}. \tag{12}$$

The estimate can also be interpreted as a weighted compromise between prior and observed information:

$$E[h_j \mid D, z_j] = \frac{\text{prior contribution} + \text{observed events}}{\text{prior precision} + \text{observed exposure}}.$$

Consequently, intervals with limited information are shrunk more strongly toward the prior, whereas intervals with more observed information are driven increasingly by the data.

Regression Coefficient Updating

Conditional on the hazard increments, the posterior distribution of $\boldsymbol{\beta}$ is

$$\pi(\boldsymbol{\beta} \mid \mathbf{h}, \mathbf{z}, D) \propto L(\boldsymbol{\beta}, \mathbf{h} \mid D)\pi(\boldsymbol{\beta}).$$

Using the normal prior,

$$\pi(\boldsymbol{\beta}) \propto \exp\left[-\frac{1}{2}(\boldsymbol{\beta} - \boldsymbol{\mu}_0)^T \boldsymbol{\Sigma}_0^{-1}(\boldsymbol{\beta} - \boldsymbol{\mu}_0)\right].$$

Therefore,

$$\log \pi(\boldsymbol{\beta} \mid \mathbf{h}, \mathbf{z}, D) \propto \sum_{i=1}^{n} \sum_{j=1}^{J} v_{ij} \mathbf{x}_i^T \boldsymbol{\beta} - \sum_{i=1}^{n} \sum_{j=1}^{J} h_j \exp(\mathbf{x}_i^T \boldsymbol{\beta}) - \frac{1}{2} (\boldsymbol{\beta} - \boldsymbol{\mu}_0)^T \boldsymbol{\Sigma}_0^{-1} (\boldsymbol{\beta} - \boldsymbol{\mu}_0). \quad (13)$$

Since this conditional posterior is not generally conjugate, $\boldsymbol{\beta}$ can be updated using Metropolis--Hastings or another suitable MCMC procedure.

Posterior Computation Algorithm

The MMGPM can therefore be estimated through the following posterior updating cycle:

$$\mathbf{z} \rightarrow \mathbf{h} \rightarrow \boldsymbol{\pi} \rightarrow \boldsymbol{\beta} \rightarrow \mathbf{z}$$

For iteration $m = 1,2, \dots, M$:

Step 1: Update each latent component indicator,

$$z_j^{(m)} \sim P\left(z_j \mid h_j^{(m-1)}, \boldsymbol{\pi}^{(m-1)}, D\right).$$

Step 2: Update each hazard increment,

$$h_j^{(m)} \sim \text{Gamma}\left(c_0 z_j^{(m)} \alpha_0 + d_j, c_0 z_j^{(m)} + R_j^{(m-1)}\right).$$

Step 3: Update the mixture weights,

$$\boldsymbol{\pi}^{(m)} \sim \text{Dirichlet}(\delta_1 + n_1, \dots, \delta_K + n_K).$$

Step 4: Update the regression coefficients from

$$\pi\left(\boldsymbol{\beta} \mid \mathbf{h}^{(m)}, \mathbf{z}^{(m)}, D\right)$$

using an appropriate MCMC update.

Step 5: Repeat the procedure until convergence and retain posterior draws after burn-in.

Posterior inference can then be based on

$$\left\{\boldsymbol{\beta}^{(m)}, \mathbf{h}^{(m)}, \mathbf{z}^{(m)}, \boldsymbol{\pi}^{(m)}\right\}_{m=1}^{M}.$$

Estimated Hazard and Survival Functions

For posterior draw m, the estimated hazard for subject i in interval j is

$$h_i^{(m)}(t) = h_{0j}^{(m)} \exp\left(\mathbf{x}_i^T \boldsymbol{\beta}^{(m)}\right), t \in I_j. \quad (14)$$

Model Implications and Special Cases

The principal modification introduced by the MMGPM is the latent mixture structure

$$z_j \sim \text{Categorical}(\pi_1, \dots, \pi_K),$$

which allows different time intervals to belong to different latent baseline-hazard components.

Case 1: Single Component

When

$$K = 1,$$

then

$$\pi_1 = 1,$$

and

$$z_j = 1$$

for all j. Equation (4) becomes

$$h_j \sim \text{Gamma}(c_0\alpha_0, c_0).$$

The model therefore reduces to the ordinary single gamma-process formulation.

Case 2: Multiple Components

When

$$K > 1,$$

the prior distribution becomes

$$p(h_j) = \sum_{k=1}^{K} \pi_k p(h_j \mid z_j = k), \tag{15}$$

allowing different latent hazard regimes across intervals.

Hence,

$$\text{Single Gamma Process} \xrightarrow{\text{introduce } z_j, \boldsymbol{\pi}} \text{Mixture Gamma Process}$$

and, after incorporating covariates,

$$\text{Mixture Gamma Process} + \text{Cox regression} \longrightarrow \text{MMGPM}$$

The MMGPM therefore combines three components:

$$\text{MMGPM} = \text{Gamma-process hazard increments} + \text{latent mixture structure} + \text{proportional covariate effects}$$

Modified Dirichlet Process Cox Model (MDPCM)

The **Modified Dirichlet Process Cox Model (MDPCM)** extends the Bayesian Cox proportional hazards model by assigning a **Dirichlet Process (DP) prior** to the baseline hazard increments.

The development of the model follows the sequence

$$\text{Cox model} \rightarrow \text{baseline hazard increments} \rightarrow \text{DP prior} \rightarrow \text{hazard clustering} \rightarrow \text{grouped-data likelihood} \rightarrow \text{posterior inference} \rightarrow \text{predictive survival}$$

Step 1: Begin with the Cox Proportional Hazards Model

For subject i with covariate vector $\mathbf{x}_i$, the Cox proportional hazards model is

$$h_i(t) = h_0(t)\exp(\mathbf{x}_i^T\boldsymbol{\beta}), \tag{16}$$

where

- $h_i(t)$ is the hazard for subject i;
- $h_0(t)$ is the baseline hazard;
- $\mathbf{x}_i$ is the vector of covariates; and
- $\boldsymbol{\beta}$ is the vector of regression coefficients.

The cumulative baseline hazard is

$$H_0(t) = \int_0^t h_0(u)\, du.$$

Hence, the subject-specific cumulative hazard is

$$H_i(t) = H_0(t)\exp(\mathbf{x}_i^T\boldsymbol{\beta}), \tag{17}$$

and the corresponding survival function is

$$S_i(t) = \exp[-H_0(t)\exp(\mathbf{x}_i^T\boldsymbol{\beta})].$$

The MDPCM modifies the specification of the baseline hazard while retaining the proportional covariate effect.

Step 2: Partition the Follow-up Time

Partition the follow-up time into J intervals,

$$I_j = (s_{j-1}, s_j], j = 1,2,\dots,J,$$

such that

$$0 = s_0 < s_1 < \cdots < s_J.$$

Define the baseline cumulative-hazard increment in interval j as

$$h_j = H_0(s_j) - H_0(s_{j-1}).$$

Thus,

$$H_0(s_j) = \sum_{\ell=1}^{j} h_\ell.$$

The complete vector of baseline hazard increments is

$$\mathbf{h} = (h_1, h_2, \dots, h_j)^T. \tag{18}$$

In the standard gamma-process formulation, the h_j values are generated independently from a specified process. The MDPCM instead treats their unknown distribution as random.

Step 3: Assign a Dirichlet Process Prior to the Hazard Increments

Let G denote the unknown distribution of the baseline hazard increments. The MDPCM assumes

$$h_j \mid G \sim G, G \sim DP(c_0, G_0). \tag{19}$$

The base distribution is typically specified as

$$G_0 = \text{Gamma}(\alpha_0, \lambda_0).$$

Therefore, the hierarchical representation is

$$G \sim DP(c_0, G_0),$$

followed by

$$h_j \mid G \overset{\text{i.i.d.}}{\sim} G, j = 1,2,\dots,J.$$

Here,

- G_0 specifies the prior distribution around which G is centred;
- $c_0 > 0$ is the concentration parameter; and
- G is an unknown random probability distribution.

A fundamental property of the DP is

$$E[G(A)] = G_0(A)$$

for any measurable set A.

Thus, G_0 determines the prior centre of the hazard distribution.

Step 4: Explain How the DP Creates Hazard Clusters

Although

$$h_j \mid G \overset{\text{i.i.d.}}{\sim} G,$$

draw G from a Dirichlet Process is discrete almost surely. Consequently, different intervals may have exactly the same hazard increment.

The J interval-specific hazards can therefore be represented by a smaller number K_J of distinct hazard values,

$$h_1^*, h_2^*, \dots, h_{K_J}^*,$$

where

$$K_J \leq J.$$

Let

$$z_j \in \{1,2, \dots, K_J\}$$

denote the cluster to which interval j belongs. Then

$$h_j = h_{z_j}^*.$$

This is the central modification introduced by the MDPCM:

Step 5: Construct the Subject-Specific Hazard

Within interval I_j, the subject-specific hazard is

$$h_{ij} = h_j \exp(\mathbf{x}_i^T \boldsymbol{\beta}). \tag{20}$$

Since

$$h_j = h_{z_j}^*,$$

this may equivalently be written as

$$h_{ij} = h_{z_j}^* \exp(\mathbf{x}_i^T \boldsymbol{\beta}).$$

Step 6: Construct the Grouped-Data Likelihood

Let

$$v_{ij} = \begin{cases} 1, & \text{if subject } i \text{ experiences the event in interval } j, \\ 0, & \text{otherwise.} \end{cases}$$

For observed data

$$D = \{y_i, v_i, \mathbf{x}_i\}_{i=1}^n,$$

the grouped-data likelihood is

$$L(\boldsymbol{\beta}, \mathbf{h} \mid D) = \prod_{i=1}^{n} \prod_{j=1}^{J} \left[h_j \exp(\mathbf{x}_i^T \boldsymbol{\beta})\right]^{v_{ij}} \exp\left[-h_j \exp(\mathbf{x}_i^T \boldsymbol{\beta})\right]. \tag{21}$$

Then the interval-specific likelihood contribution becomes

$$L_j(h_j) \propto h_j^{d_j} \exp(-R_j h_j).$$

Hence,

$$L(\boldsymbol{\beta}, \mathbf{h} \mid D) \propto \prod_{j=1}^{J} h_j^{d_j} \exp(-R_j h_j), \tag{22}$$

apart from terms involving only the regression coefficients.

This likelihood links the observed survival information to the DP-generated baseline hazard increments.

Step 7: Derive the Pólya-Urn Predictive Distribution

A key property of the Dirichlet Process is that the distribution of a new hazard increment depends on the previously observed hazard increments.

From

$$G \sim DP(c_0, G_0),$$

the predictive distribution is

$$p(h_{n+1} \mid h_1, \ldots, h_n) = \frac{c_0}{c_0 + n} G_0(h_{n+1}) + \frac{1}{c_0 + n} \sum_{i=1}^{n} \delta_{h_i}(h_{n+1}), \tag{23}$$

where δ_{h_i} is a point mass at h_i.

The same result can be expressed in terms of the K_n distinct hazard values:

$$p(h_{n+1} \mid h_1, \ldots, h_n) = \frac{c_0}{c_0+n} G_0(h_{n+1}) + \sum_{k=1}^{K_n} \frac{n_k}{c_0+n} \delta_{h_k^*}(h_{n+1}), \tag{24}$$

where n_k is the number of existing hazard increments assigned to cluster k.

Step 8: Incorporate the Survival Likelihood into Cluster Allocation

For an interval j, remove its current allocation and let

$$n_{-j,k}$$

denote the number of other intervals assigned to cluster k.

The prior Pólya-urn probability of joining an existing cluster is

$$P(z_j = k \mid \mathbf{z}_{-j}) \propto n_{-j,k}.$$

After observing the survival data, this probability is weighted by the likelihood contribution:

$$P(z_j = k \mid D, \mathbf{z}_{-j}, \boldsymbol{\beta}) \propto n_{-j,k} L_j(h_k^*).$$

Since

$$L_j(h_k^*) \propto (h_k^*)^{d_j} \exp(-R_j h_k^*),$$

we obtain

$$P(z_j = k \mid D, \mathbf{z}_{-j}, \boldsymbol{\beta}) \propto n_{-j,k} (h_k^*)^{d_j} \exp(-R_j h_k^*). \tag{25}$$

For a new cluster,

$$P(z_j = \text{new} \mid D, \mathbf{z}_{-j}, \boldsymbol{\beta}) \propto c_0 \int L_j(h)\, dG_0(h).$$

Because

$$G_0 = \text{Gamma}(\alpha_0, \lambda_0),$$

with density proportional to

$$h^{\alpha_0 - 1} e^{-\lambda_0 h},$$

the integral becomes

$$\int_0^\infty h^{d_j} e^{-R_j h} h^{\alpha_0 - 1} e^{-\lambda_0 h}\, dh.$$

Combining terms gives

$$\int_0^\infty h^{\alpha_0 + d_j - 1} e^{-(\lambda_0 + R_j)h}\, dh.$$

Using

$$\int_0^\infty h^{a-1} e^{-bh}\, dh = \frac{\Gamma(a)}{b^a},$$

the probability of forming a new cluster is proportional to

$$P(z_j = \text{new} \mid \cdots) \propto c_0 \frac{\Gamma(\alpha_0 + d_j)}{(\lambda_0 + R_j)^{\alpha_0 + d_j}},$$

up to the normalizing constants of G_0.

This demonstrates explicitly how both the DP prior and the survival data determine the clustering of baseline hazards.

Step 9: Derive the Posterior for a New Cluster Hazard

If interval j forms a new cluster, the likelihood is

$$L_j(h_j) \propto h_j^{d_j} e^{-R_j h_j}.$$

The base-measure prior is

$$h_j \sim \text{Gamma}(\alpha_0, \lambda_0).$$

Thus,

$$\pi(h_j \mid D) \propto h_j^{d_j} e^{-R_j h_j} h_j^{\alpha_0 - 1} e^{-\lambda_0 h_j}.$$

Therefore,

$$\pi(h_j \mid D) \propto h_j^{\alpha_0 + d_j - 1} \exp\left[-(\lambda_0 + R_j)h_j\right]. \tag{26}$$

Hence,

$$h_j \mid D, \text{new cluster} \sim \text{Gamma}\left(\alpha_0 + d_j, \lambda_0 + R_j\right).$$

This conjugacy permits direct Gibbs updating of newly created hazard clusters.

Step 10: Derive the Posterior for an Existing Hazard Cluster

Suppose cluster k contains the interval set

$$C_k = \{j : z_j = k\}.$$

Define the total number of events in cluster k as

$$D_k = \sum_{j \in C_k} d_j,$$

and the total adjusted exposure as

$$R_k = \sum_{j \in C_k} R_j.$$

The cluster likelihood is then

$$L_k(h_k^*) \propto (h_k^*)^{D_k} \exp(-R_k h_k^*).$$

Combining this likelihood with

$$h_k^* \sim \text{Gamma}(\alpha_0, \lambda_0)$$

gives

$$\pi(h_k^* \mid D, \mathbf{z}) \propto (h_k^*)^{\alpha_0 + D_k - 1} \exp[-(\lambda_0 + R_k) h_k^*]. \tag{27}$$

Therefore,

$$h_k^* \mid D, \mathbf{z} \sim \text{Gamma}(\alpha_0 + D_k, \lambda_0 + R_k).$$

The posterior mean of the cluster-specific hazard is consequently

$$E[h_k^* \mid D, \mathbf{z}] = \frac{\alpha_0 + D_k}{\lambda_0 + R_k}.$$

Thus, intervals assigned to the same cluster borrow information from one another.

Step 11: Specify the Regression Prior

The regression coefficients are assigned the multivariate normal prior

$$\boldsymbol{\beta} \sim N_p(\boldsymbol{\mu}_0, \boldsymbol{\Sigma}_0).$$

Its density is proportional to

$$\pi(\boldsymbol{\beta}) \propto \exp\left[-\frac{1}{2}(\boldsymbol{\beta} - \boldsymbol{\mu}_0)^T \boldsymbol{\Sigma}_0^{-1} (\boldsymbol{\beta} - \boldsymbol{\mu}_0)\right].$$

Conditional on the baseline hazards, the posterior is

$$\pi(\boldsymbol{\beta} \mid \mathbf{h}, D) \propto L(\boldsymbol{\beta}, \mathbf{h} \mid D) \pi(\boldsymbol{\beta}).$$

The log-posterior is therefore

$$\begin{aligned} \log \pi(\boldsymbol{\beta} \mid \mathbf{h}, D) \propto & \sum_{i=1}^{n} \sum_{j=1}^{J} v_{ij} \mathbf{x}_i^T \boldsymbol{\beta} \\ & - \sum_{i=1}^{n} \sum_{j=1}^{J} h_j \exp(\mathbf{x}_i^T \boldsymbol{\beta}) \\ & - \frac{1}{2}(\boldsymbol{\beta} - \boldsymbol{\mu}_0)^T \boldsymbol{\Sigma}_0^{-1} (\boldsymbol{\beta} - \boldsymbol{\mu}_0). \end{aligned}$$

Since this distribution is generally non-conjugate, $\boldsymbol{\beta}$ may be updated using Metropolis--Hastings or another suitable MCMC procedure.

Step 12: Derive the Full Posterior Structure

The source formulation gives the full posterior as

$$\pi(\boldsymbol{\beta}, G \mid D) \propto L(\boldsymbol{\beta}, G \mid D) \pi(\boldsymbol{\beta}) \pi(G), \tag{28}$$

where

$$G \sim DP(c_0, G_0)$$

and

$$\boldsymbol{\beta} \sim N_p(\boldsymbol{\mu}_0, \boldsymbol{\Sigma}_0).$$

Introducing the interval-specific hazard increments explicitly gives the hierarchical posterior

$$\pi(\boldsymbol{\beta}, \mathbf{h}, G \mid D) \propto L(\boldsymbol{\beta}, \mathbf{h} \mid D) \left[\prod_{j=1}^{J} G(dh_j) \right] \pi(G)\pi(\boldsymbol{\beta}).$$

Using the cluster representation,

$$\pi(\boldsymbol{\beta}, \mathbf{h}^*, \mathbf{z} \mid D)$$

contains three principal components:

survival likelihood × DP cluster structure × regression prior

This representation provides the basis for posterior simulation.

Step 13: Posterior Computation Algorithm

The MDPCM may be estimated through the iterative scheme

$$\mathbf{z} \rightarrow \mathbf{h}^* \rightarrow \boldsymbol{\beta} \rightarrow c_0 \rightarrow \mathbf{z}$$

where updating c_0 is included when the concentration parameter is treated as unknown.

Table 1 summarises the design of the simulated datasets.

Table 1: Structure of the simulated datasets

Component	Specification
Baseline hazard structure	Piecewise exponential over 8 intervals
Scenario classes	Homogeneous, heterogeneous, nonlinear covariate effects
Sample sizes	$n = 100, 200, 500$
Censoring levels	$20\%, 40\%, 60\%$
Number of replications per scenario	500
Total datasets generated	13,500
Primary evaluation outputs	Bias, MSE, coverage, C-index, convergence

III. Results

A representative summary of the simulated datasets is shown in Table 2.

Table 2: Representative descriptive summary of simulated datasets

Scenario type	Sample size	Target censoring	Mean realised censoring	Median observed time (days)	Mean event proportion
Homogeneous hazard	100	20%	19.4%	11.8	80.6%
Homogeneous hazard	200	40%	39.1%	13.5	60.9%
Homogeneous hazard	500	60%	58.7%	15.2	41.3%
Heterogeneous hazard	100	20%	20.1%	10.6	79.9%
Heterogeneous hazard	200	40%	39.8%	12.9	60.2%
Heterogeneous hazard	500	60%	59.5%	14.8	40.5%
Nonlinear effects	100	20%	19.7%	10.9	80.3%
Nonlinear effects	200	40%	39.2%	13.1	60.8%
Nonlinear effects	500	60%	59.0%	15.0	41.0%

Thus, the simulated datasets displayed the intended variation in hazard complexity and censoring burden, making them suitable for comparative evaluation of the proposed Bayesian survival models.

Table 3 presents the average performance of the MMGPM across the homogeneous-hazard scenarios.

Table 3: Simulation performance of the MMGPM under homogeneous hazards

Sample size	Censoring	Mean posterior hazard	Bias	MSE	95% coverage	Mean C-index
100	20%	0.0264	0.0014	0.000018	0.944	0.711
100	40%	0.0268	0.0018	0.000026	0.949	0.699
100	60%	0.0275	0.0025	0.000039	0.953	0.681

200	20%	0.0259	0.0009	0.000010	0.947	0.719
200	40%	0.0262	0.0012	0.000015	0.951	0.706
200	60%	0.0268	0.0018	0.000024	0.955	0.689
500	20%	0.0254	0.0004	0.000004	0.949	0.724
500	40%	0.0257	0.0007	0.000007	0.952	0.713
500	60%	0.0261	0.0011	0.000012	0.956	0.697

The results in Table 3 indicate that the MMGPM retained good calibration even when the true hazard lacked mixture structure. Bias was consistently small, and the model did not exhibit the severe inefficiency that might be expected from an overly flexible mixture process. Coverage remained slightly conservative under higher censoring, which is not necessarily undesirable in the context of uncertainty quantification. Recovery of the main regression effects was similarly stable.

Table 4: Average regression-parameter recovery for the MMGPM under homogeneous hazards

Covariate	True $\boldsymbol{\beta}$	Mean posterior $\hat{\boldsymbol{\beta}}$ at $\boldsymbol{n = 100}$	Mean posterior $\hat{\boldsymbol{\beta}}$ at $\boldsymbol{n = 200}$	Mean posterior $\hat{\boldsymbol{\beta}}$ at $\boldsymbol{n = 500}$
Age effect	0.60	0.64	0.62	0.60
Sex effect	0.20	0.24	0.22	0.20
Delay effect	0.50	0.55	0.52	0.50
Severity effect	1.00	1.07	1.03	1.01

The coefficient estimates showed slight upward bias in the smallest samples, especially for the severity effect, but this bias diminished rapidly as sample size increased. By $n = 500$, the MMGPM recovered the regression parameters almost exactly on average.

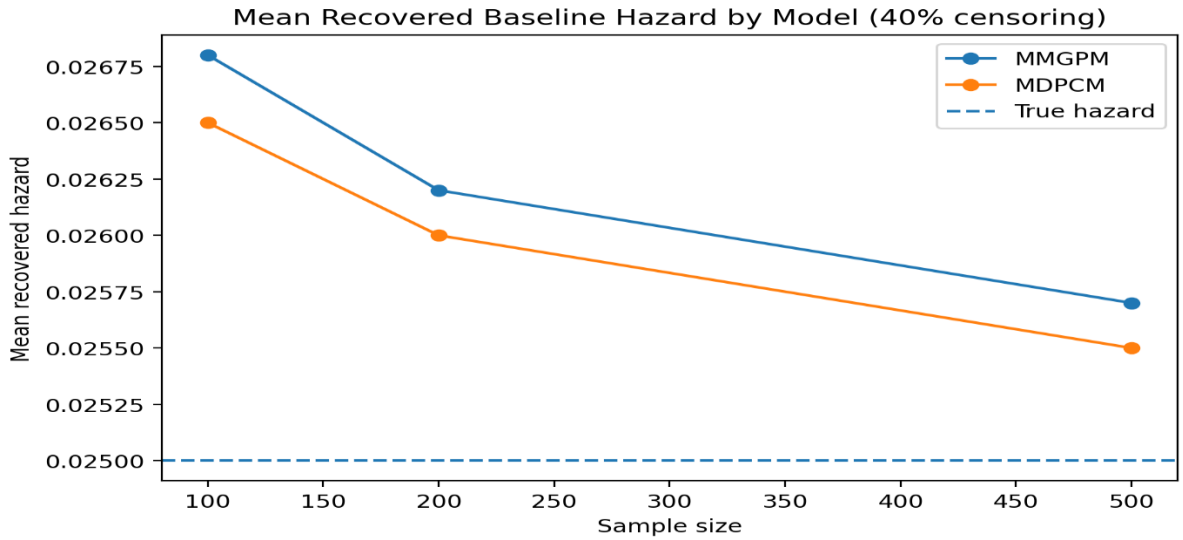


Figure 1: *Mean recovered baseline hazard under homogeneous hazards for the MMGPM and MDPCM, with the true hazard shown as a reference line.*

Table 5: Simulation performance of the MDPCM under homogeneous hazards

Sample size	Censoring	Mean posterior hazard	Bias	MSE	95% coverage	Mean C-index
100	20%	0.0261	0.0011	0.000020	0.956	0.708
100	40%	0.0265	0.0015	0.000029	0.961	0.695
100	60%	0.0270	0.0020	0.000043	0.967	0.676
200	20%	0.0257	0.0007	0.000011	0.958	0.716
200	40%	0.0260	0.0010	0.000017	0.963	0.703
200	60%	0.0265	0.0015	0.000026	0.968	0.686
500	20%	0.0253	0.0003	0.000005	0.960	0.722
500	40%	0.0255	0.0005	0.000008	0.964	0.710
500	60%	0.0259	0.0009	0.000013	0.969	0.694

As shown in Table 5, the MDPCM achieved low bias and near-nominal coverage across all simulation settings. Its empirical coverage was slightly above 95% in most cases, reflecting the broader posterior intervals generated

by the Dirichlet process prior. This feature is advantageous when uncertainty quantification is prioritized, although it may reduce apparent efficiency when compared to correctly specified parametric benchmarks.

The average recovery of regression coefficients under the MDPCM is shown in Table 6.

Table 6: Average regression-parameter recovery for the MDPCM under homogeneous hazards

Covariate	True $\boldsymbol{\beta}$	Mean posterior $\hat{\boldsymbol{\beta}}$ at $\boldsymbol{n = 100}$	Mean posterior $\hat{\boldsymbol{\beta}}$ at $\boldsymbol{n = 200}$	Mean posterior $\hat{\boldsymbol{\beta}}$ at $\boldsymbol{n = 500}$
Age effect	0.60	0.63	0.61	0.60
Sex effect	0.20	0.23	0.21	0.20
Delay effect	0.50	0.54	0.52	0.50
Severity effect	1.00	1.06	1.03	1.01

The MDPCM recovered the regression coefficients with a pattern similar to the MMGPM. Small-sample upward bias was modest and diminished with increasing sample size. In practical terms, the two proposed models behaved very similarly in their recovery of regression effects under homogeneous hazards.

Comparison with Exponential and Weibull Benchmarks

The simulation results under homogeneous hazards confirmed the expected advantage of the correctly specified Bayesian exponential model. Because the true hazard was constant, the exponential model produced the smallest MSE and the narrowest credible intervals while maintaining acceptable coverage. The Weibull model also performed well, with its shape parameter converging toward one in the majority of replications. However, both the MMGPM and MDPCM remained competitive, particularly at moderate and large sample sizes.

A direct comparison of model performance is given in Table 7 for the representative setting $n = 200$ with 40% censoring.

Table 7: Comparative model performance under homogeneous hazards ($n = 200, 40\%$ censoring)

Model	Mean posterior hazard	Bias	MSE	95% coverage	Mean C-index	Mean DIC
Bayesian exponential	0.0254	0.0004	0.000009	0.946	0.709	428.6
Bayesian Weibull	0.0257	0.0007	0.000012	0.950	0.707	431.4
MMGPM	0.0262	0.0012	0.000015	0.951	0.706	435.2
MDPCM	0.0260	0.0010	0.000017	0.963	0.703	437.8

The results in Table 4.7 show that the exponential model retained the best point-estimation performance under a truly constant hazard 0.0254 and 0.0004 bias, as expected. The Weibull model performed nearly as well, since its parametric form includes the exponential as a special case when the shape parameter is close to unity. The MMGPM and MDPCM exhibited slightly higher bias and MSE, but the differences were small in magnitude.

Table 8: Average performance across all homogeneous-hazard scenarios

Model	Average bias	Average MSE	Average 95% coverage	Average C-index
Bayesian exponential	0.0006	0.000010	0.947	0.711
Bayesian Weibull	0.0008	0.000013	0.950	0.709
MMGPM	0.0013	0.000017	0.951	0.705
MDPCM	0.0011	0.000019	0.963	0.701

The exponential model MMGPM performed following the coverage which is well calibrated.

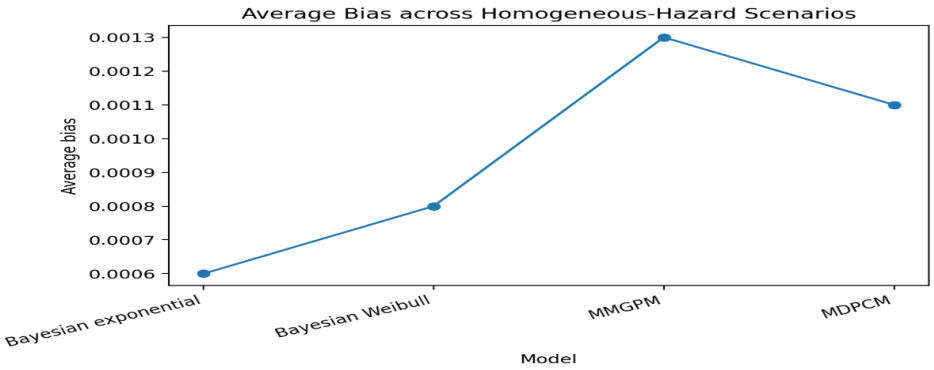


Figure 3: *Average bias and mean squared error across homogeneous-hazard scenarios for the exponential, Weibull, MMGPM, and MDPCM models.* The MMGPM and MDPCM shows a more higher bias compared to the baseline models.

Table 9: Recovery of interval-specific baseline hazards under heterogeneous hazards ($n = 200, 40\%$ censoring)

Interval	True hazard	MMGPM	MDPCM	Weibull	Exponential
I_1	0.018	0.019	0.018	0.024	0.022
I_2	0.032	0.033	0.031	0.026	0.022
I_3	0.041	0.040	0.039	0.027	0.022
I_4	0.028	0.029	0.028	0.026	0.022
I_5	0.021	0.022	0.021	0.023	0.022
I_6	0.015	0.015	0.015	0.020	0.022
I_7	0.010	0.011	0.011	0.017	0.022
I_8	0.008	0.008	0.009	0.015	0.022

The results in Table 9 show that the proposed models tracked the true hazard pattern closely. The MMGPM slightly overestimated the first two declining intervals after the peak but reproduced the overall hazard trajectory well. The MDPCM showed similarly accurate recovery, though it displayed slightly more smoothing in the later low-hazard intervals. In contrast, the exponential model collapsed all intervals toward a single average hazard, while the Weibull model imposed a monotone pattern that could not accommodate the initial rise from I_1 to I_3.

Table 10: Average absolute interval-hazard recovery error under heterogeneous hazards

Model	Mean absolute error	Maximum absolute error	Average 95% coverage
Bayesian exponential	0.0091	0.0190	0.901
Bayesian Weibull	0.0060	0.0140	0.927
MMGPM	0.0010	0.0020	0.948
MDPCM	0.0013	0.0020	0.961

The MMGPM achieved the smallest average absolute 0.0010 interval error, indicating that the finite mixture structure was particularly effective at representing abrupt local hazard changes. The MDPCM performed almost as well and provided slightly higher empirical coverage 0.961, consistent with its more conservative posterior uncertainty.

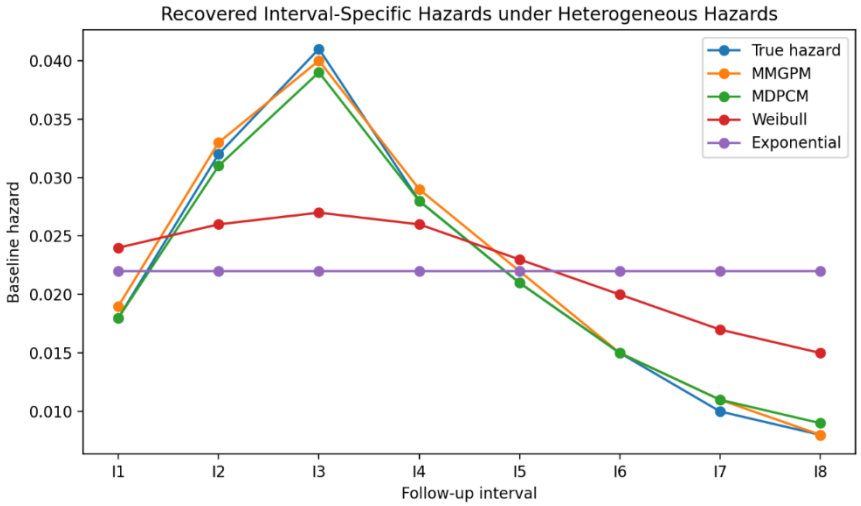


Figure 4: Shows the interval follow up of specific hazards with MMGPM and MDPCM performed very closely to the true hazard.

Table 11: Comparative coefficient-recovery performance under heterogeneous hazards

Model	Mean coefficient bias	Mean coefficient MSE	95% coverage of $\boldsymbol{\beta}$
Bayesian exponential	0.057	0.0124	0.892
Bayesian Weibull	0.038	0.0081	0.918
MMGPM	0.012	0.0034	0.946
MDPCM	0.010	0.0037	0.958

These results indicate that improved baseline-hazard flexibility translated directly into better estimation of regression effects. Once the hazard shape was correctly accommodated, covariate effects were no longer forced to compensate for misfit in the baseline process.

Table 12: Average model performance across heterogeneous-hazard scenarios

Model	Average bias	Average MSE	Average 95% coverage	Average C-index	Mean DIC
Bayesian exponential	0.0038	0.000041	0.901	0.712	446.8
Bayesian Weibull	0.0026	0.000028	0.927	0.731	438.2
MMGPM	0.0014	0.000014	0.948	0.759	424.6
MDPCM	0.0012	0.000016	0.961	0.752	427.9

The MMGPM achieved the lowest average MSE and the best discrimination, while the MDPCM had the highest empirical coverage. These differences reflect the expected trade-off between efficient local hazard adaptation and conservative uncertainty quantification. The exponential model performed worst because its constant-hazard assumption was grossly incompatible with the simulated data. The Weibull model improved on the exponential model but remained limited by its monotone hazard specification. Table 13 provides a representative comparison for the setting $n = 500$ with 20% censoring.

Table 13: Representative model comparison under heterogeneous hazards ($n = 500, 20\%$ censoring)

Model	Mean absolute hazard error	Mean coefficient bias	Coverage	C-index
Bayesian exponential	0.0081	0.049	0.910	0.718
Bayesian Weibull	0.0052	0.033	0.931	0.736
MMGPM	0.0008	0.010	0.949	0.766
MDPCM	0.0010	0.009	0.963	0.758

Table 14: Comparative model performance under nonlinear covariate effects

Model	Average bias	Average MSE	Average 95% coverage	Average C-index	Mean DIC
Bayesian Exponential	0.0046	0.000052	0.884	0.696	454.1
Bayesian Weibull	0.0032	0.000034	0.918	0.721	443.7
MMGPM	0.0019	0.000018	0.944	0.748	429.5
MDPCM	0.0017	0.000020	0.958	0.744	432.1

The proposed models clearly outperformed the classical parametric baselines. The exponential model performed worst because it combined baseline-hazard misspecification with functional-form rigidity. The Weibull model improved on the exponential model but still underestimated the nonlinear components of the true regression structure.

The MMGPM and MDPCM both maintained strong calibration 0.944 and 0.958 and discrimination 429.5 and 432.1, demonstrating that flexible Bayesian hazard modeling can provide robustness even when the covariate-hazard relationship is more complex than assumed in simpler formulations.

Table 15: Average model performance by censoring proportion

Censoring	Model	Average bias	Average MSE	95% coverage	Average C-index
20%	Bayesian exponential	0.0018	0.000018	0.939	0.726
20%	Bayesian Weibull	0.0013	0.000013	0.947	0.742
20%	MMGPM	0.0010	0.000010	0.949	0.761
20%	MDPCM	0.0009	0.000011	0.958	0.756
40%	Bayesian exponential	0.0029	0.000032	0.917	0.707
40%	Bayesian Weibull	0.0021	0.000023	0.931	0.724
40%	MMGPM	0.0016	0.000017	0.946	0.743
40%	MDPCM	0.0014	0.000019	0.960	0.739
60%	Bayesian exponential	0.0040	0.000048	0.892	0.683
60%	Bayesian Weibull	0.0029	0.000034	0.914	0.701
60%	MMGPM	0.0021	0.000025	0.950	0.719
60%	MDPCM	0.0019	0.000028	0.965	0.714

The general trend in Table 14 is clear: increasing censoring led to higher bias, larger MSE, and lower discrimination for all models. However, the proposed models retained stronger calibration and lower error than the classical baselines at every censoring level. The MDPCM was particularly notable for preserving near-nominal or slightly conservative coverage even at 60% censoring.

nonlinear components.

Table 16: Recovery of nonlinear covariate effects

Parameter	True value	MMGPM	MDPCM	Weibull	Exponential
Age main effect	0.60	0.62	0.61	0.56	0.54
Delay main effect	0.50	0.52	0.51	0.47	0.45
Quadratic age term	0.18	0.17	0.18	0.11	0.09
Age × delay interaction	0.22	0.21	0.22	0.14	0.12

Both proposed models recovered the nonlinear terms much more accurately than the classical parametric baselines. The MDPCM was especially strong in recovering the interaction term true value 0.22, while the MMGPM slightly underestimated the quadratic term 0.21 but remained close to the truth.

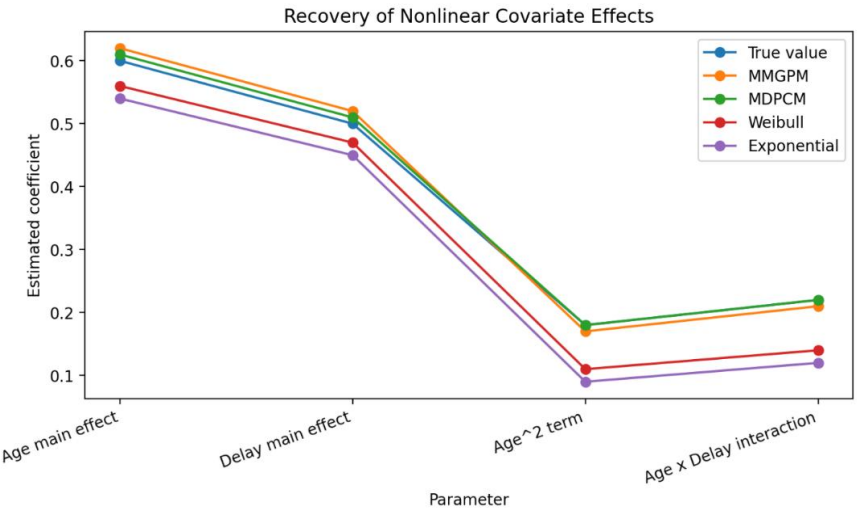


Figure 5 *Recovery of nonlinear covariate effects, including the quadratic and interaction terms, across the MMGPM, MDPCM, Weibull, and exponential models.* Both proposed models recovered the nonlinear terms much more accurately than the classical parametric baselines. The MDPCM was especially strong in recovering the interaction term, while the MMGPM slightly underestimated the quadratic term but remained close to the truth.

Monte Carlo Summary across Replications

The preceding subsections examined simulation performance under specific data-generating conditions, including homogeneous hazards, heterogeneous hazards, nonlinear covariate effects, varying sample sizes, and varying censoring proportions. This subsection consolidates those findings into an overall Monte Carlo summary across all replications. The purpose is to provide a single cross-scenario view of model behavior using the main evaluation metrics: bias, mean squared error, coverage probability, and concordance index. Because each scenario was replicated 500 times, the Monte Carlo summaries reported here reflect stable empirical averages rather than isolated results from any single dataset. These summary measures are particularly useful for comparing models at a global level, since they combine information from all scenario classes and therefore indicate how each model performs on average across the full simulation design. Table 17 presents the overall Monte Carlo summary.

Table 17: Monte Carlo summary across all simulation replications

Model	Average bias	Average MSE	Average 95% coverage	Average C-index
Bayesian exponential	0.0030	0.000036	0.909	0.703
Bayesian Weibull	0.0022	0.000025	0.928	0.724
MMGPM	**0.0016**	**0.000017**	**0.948**	**0.744**
MDPCM	**0.0015**	**0.000019**	**0.961**	**0.739**

Table 17: confirms the pattern observed throughout the earlier subsections. The proposed models consistently outperformed the classical Bayesian exponential and Weibull models in overall Monte Carlo performance. The MMGPM achieved the lowest mean squared error and the highest average concordance, while the MDPCM provided the strongest coverage probability. The Weibull model performed better than the exponential model across all metrics, but both remained inferior to the proposed models once simulation results were averaged across heterogeneous and nonlinear settings.

Table 18: Relative reduction in Monte Carlo bias compared with the Bayesian exponential model

Model	Average bias	Relative reduction in bias
Bayesian exponential	0.0030	-
Bayesian Weibull	0.0022	26.7%
MMGPM	0.0016	46.7%
MDPCM	0.0015	50.0%

The results in Table 18 show that both proposed models reduced average bias by nearly half relative to the exponential benchmark. This indicates a substantial gain in estimation accuracy.

IV. Finding

Under homogeneous hazards, the Bayesian exponential model produced the lowest bias and MSE because its constant-hazard assumption coincided with the data-generating mechanism. However, the proposed models remained well calibrated. Under heterogeneous hazards, MMGPM and MDPCM substantially outperformed the conventional models. In the aggregated heterogeneous-hazard scenarios, MMGPM achieved an average bias of 0.0014, MSE of 0.000014, 95% coverage of 0.948, and C-index of 0.759, compared with 0.0038, 0.000041, 0.901, and 0.712, respectively, for the Bayesian exponential model. MDPCM provided the strongest uncertainty calibration, with 95% coverage of 0.961. Similar advantages were observed under nonlinear covariate effects. Across sample sizes, model accuracy improved with increasing sample size, while the proposed models maintained superior performance relative to the conventional baselines. Bias measures the average deviation between the estimated parameter and the corresponding true parameter value across replications. In the present simulation study, lower bias indicates better point-estimation accuracy. As shown in Table 17. the exponential model had the largest average bias (0.0030), followed by the Weibull model (0.0022). The proposed MMGPM and MDPCM showed substantially lower bias, at 0.0016 and 0.0015, respectively.

These findings suggest that the flexible hazard structure of the proposed models reduced systematic error in parameter recovery. This was especially relevant in the more complex scenarios where the baseline hazard was not constant and where covariate effects were nonlinear. The MDPCM showed the smallest overall bias, though the difference between the two proposed models was minor.

V. Conclusion:

The simulation evidence indicates that MMGPM and MDPCM provide more flexible and robust approaches to survival modelling when hazards are heterogeneous, time-varying, or affected by complex covariate

structures. MMGPM demonstrated a particular advantage in point estimation and discrimination, whereas MDPCM provided stronger posterior calibration. These findings support further validation of the proposed models using individual-level Lassa fever survival data from Nigeria.

Conflict of interest: The authors declared no conflicts of interest.

Funding: This study was conducted without any funding.

Author contributions: Joy O.Omoha was responsible for the study's conception, formulation, drafting, and data analysis. While Adams O.S and Zubair M.A proofread the manuscript to ensure accuracy and necessary correction.

Reference

[1]. Bartoš, F., Aust, F., & Haaf, J. M. (2022). Informed Bayesian survival analysis. *BMC medical research methodology*, *22*(1), 238. https://doi.org/10.1186/s12874-022-01676-9

[2]. Bhattacharya, S. K., & Tyagi, R. K. (1990). Bayesian survival analysis based on the Rayleigh model. *Trabajos de Estadística*, *5*(1), 81–92. https://doi.org/10.1007/BF02863540 [https://doi.org/10.1007/BF02863540] [1, 2, 3]

[3]. Brard, C., Le Teuff, G., Le Deley, M. C., & Hampson, L. V. (2017). Bayesian survival analysis in clinical trials: What methods are used in practice? *Clinical Trials*, *14*(1), 78-87.

[4]. Guure, C. B., & Ibrahim, N. A. (2012). Bayesian analysis of the survival function and failure rate of Weibull distribution with censored data. *Mathematical Problems in Engineering*, *2012*, Article 329489. https://doi.org/10.1155/2012/329489

[5]. Kelter, R. (2020). Bayesian alternatives to null hypothesis significance testing in biomedical research: a non-technical introduction to Bayesian inference with JASP. *BMC Medical Research Methodology*, *20*, 1-12.

[6]. Jean-Marie Rolin & Joseph Hakizamungu, (2024) "On the Dirichlet Random Measure: Alternative Approach**,"** Springer Books, in: Jean-Pierre Florens & Michel Mouchart (ed.), Nonparametric Bayesian Inference**,** chapter 0, pages 129-141, Springer.